Zhu *et al. Metab Target Organ Damage.* 2025;5:29
DOI: 10.20517/mtod.2025.47

Metabolism and Target Organ Damage

Original Article

Open Access

Check for updates

Bilirubin ameliorates metabolic dysregulation by targeting the HSP90β/SREBPs signaling axis to improve insulin resistance and mitigate ectopic lipid deposition

Jing Zhu[1,#], Hai-Tao Xiao[2,#], Qiu-Yi Wu[2], Xue-Xue Shao[2], Yu-Fan Meng[2], Jie-Xia Ding[1], Jia-Xin He[2], Li-Na Lai[3], Ning Xue[4], Zu-Guo Zheng[2]

[1]Department of Infectious Diseases, Hangzhou First People's Hospital, Hangzhou 310006, Zhejiang, China.
[2]State Key Laboratory of Natural Medicines, School of Traditional Chinese Pharmacy, China Pharmaceutical University, Nanjing 210009, Jiangsu, China.
[3]School of Pharmacy, Changzhi Medical College, Changzhi 046000, Shanxi, China.
[4]Department of Acupuncture, Jurong Hospital Affiliated to Jiangsu University, Zhenjiang 212400, Jiangsu, China.

Correspondence to: Prof. Ning Xue, Department of Acupuncture, Jurong Hospital Affiliated to Jiangsu University, No. 66 Ersheng Road, Zhenjiang 212400, Jiangsu, China. E-mail: enderxx@126.com; Prof. Zu-Guo Zheng, State Key Laboratory of Natural Medicines, School of Traditional Chinese Pharmacy, China Pharmaceutical University, No. 601 Tongjia Lane, Nanjing 210009, Jiangsu, China. E-mail: zuguozheng@cpu.edu.cn

How to cite this article: Zhu J, Xiao HT, Wu QY, Shao XX, Meng YF, Ding JX, He JX, Lai LN, Xue N, Zheng ZG. Bilirubin ameliorates metabolic dysregulation by targeting the HSP90β/SREBPs signaling axis to improve insulin resistance and mitigate ectopic lipid deposition. *Metab Target Organ Damage.* 2025;5:29. https://dx.doi.org/10.20517/mtod.2025.47

Received: 11 Apr 2025 **First Decision:** 14 May 2025 **Revised:** 26 Jun 2025 **Accepted:** 30 Jun 2025 **Published:** 30 Jun 2025

Academic Editor: Amedeo Lonardo **Copy Editor:** Ting-Ting Hu **Production Editor:** Ting-Ting Hu

Abstract

Aim: Sterol regulatory element-binding proteins (SREBPs) are key transcription factors driving *de novo* lipid synthesis (DNL) and associated metabolic disorders. This study aims to investigate whether bilirubin, a potential SREBP inhibitor, alleviates lipid accumulation and insulin resistance by targeting the HSP90β/SREBP pathway.

Methods: *In vitro*, HL-7702 cells were treated with bilirubin to assess lipid-lowering effects and SREBP-related gene expression. *In vivo*, high-fat diet (HFD)-induced obese mice received bilirubin intervention for 6 weeks. Lipid profiles, insulin sensitivity, hepatic SREBP protein levels, and downstream gene expression were analyzed. Mechanistic studies focused on HSP90β activity modulation by bilirubin.

Results: Bilirubin significantly reduced lipid accumulation in HL-7702 cells and downregulated SREBPs and their

© The Author(s) 2025. **Open Access** This article is licensed under a Creative Commons Attribution 4.0 International License (https://creativecommons.org/licenses/by/4.0/), which permits unrestricted use, sharing, adaptation, distribution and reproduction in any medium or format, for any purpose, even commercially, as long as you give appropriate credit to the original author(s) and the source, provide a link to the Creative Commons license, and indicate if changes were made.

target genes. In HFD-fed mice, bilirubin attenuated obesity, hepatic steatosis, and insulin resistance, accompanied by suppressed SREBP protein levels and expression of target genes. Mechanistically, bilirubin inhibited SREBP activation by targeting HSP90β.

Conclusion: Bilirubin ameliorates metabolic syndrome via the HSP90β/SREBP axis, providing a novel therapeutic strategy for lipid metabolism disorders and insulin resistance. These findings highlight bilirubin's potential as a pharmacological agent against metabolic diseases.

Keywords: Bilirubin, metabolic syndrome, SREBPs, HSP90β

INTRODUCTION

Metabolic syndrome represents a cluster of interrelated pathological conditions that collectively elevate cardiovascular risk, including central adiposity, elevated blood pressure, atherogenic dyslipidemia, impaired glucose homeostasis, and hepatic steatosis[1,2]. According to WHO surveillance data, obesity has reached pandemic proportions, resulting in the deaths of at least 2.8 million individuals annually[3]. Obesity is a major factor in causing insulin resistance, cardiovascular disorders, and type 2 diabetes (T2D), which often leads to hyperglycemia and can result in complications such as hypertension, stroke, atherosclerosis, and cancer[4,5]. Obesity can weaken the body's ability to fight off harmful substances, leading to a higher risk of developing conditions that make one more susceptible to illness[6,7]. Approaches that reduce obesity offer the potential to lower death rates and enhance the well-being of those impacted.

Bilirubin represents the terminal catabolite in vertebrate heme degradation pathways. During this metabolic process, heme oxygenase isoforms (HO-1/HO-2) catalyze the oxidative cleavage of heme's tetrapyrrole structure, yielding three bioactive products: gaseous carbon monoxide, ferrous iron ions, and the intermediate biliverdin[8]. Biliverdin, which is attracted to water, is converted to bilirubin by biliverdin reductase[9]. Bilirubin, a hydrophobic tetrapyrrole compound, is both insoluble and harmful to cells, so it is transformed by uridine diphosphate glucuronosyltransferase 1A1 (UGT1A1) in the liver through glucuronidation before being released into bile[10]. Human serum bilirubin typically falls within the range of 0.1 to 1.2 mg/dL (1.71-20.52 μM)[11]. Bilirubin has been considered simply a byproduct with potential harm[12]. However, the roles of bilirubin could rely on its concentration. Several recent studies have shown the positive impact of increased bilirubin levels in the blood on different illnesses and its antioxidant properties at normal levels. Low levels of serum bilirubin, a potent antioxidant in the body, have a negative correlation with abdominal obesity, metabolic syndromes, systemic inflammation, diabetes, diabetes-related nephropathy, amputation, cardiovascular disease, endothelial dysfunction, and low-density lipoprotein oxidation[13]. Slightly increased levels of bilirubin in the bloodstream appear to be a potential focus for preventing and decreasing the occurrence of cardiovascular disease and other conditions related to oxidative stress, such as T2D and cancer[14]. Research conducted on various groups of patients has also shown an inverse correlation between levels of bilirubin in the blood and fatty liver disease. Although these studies show a connection, the reason higher levels of bilirubin in the blood provide defense against liver fat accumulation remains unclear.

Sterol regulatory element-binding proteins (SREBPs) play a significant role in maintaining lipid balance by regulating the genes responsible for producing and absorbing fatty acids, triglyceride (TG), cholesterol, and phospholipids[15]. SREBPs play a crucial role in lipid metabolism, making them closely associated with metabolic syndrome[16]. When sterol levels are low or insulin is administered, the coated protein II (COP II) vesicles facilitate the movement of SREBPs from the ER to the Golgi apparatus by controlling the interaction between SREBP cleavage-activating protein (SCAP) with insulin-induced genes (INSIGs)[17].

Within the Golgi complex, site-1 protease (S1P) and site-2 protease (S2P) consecutively cut SREBPs to produce fully developed SREBPs, which are then discharged from the Golgi complex and transported to the nucleus[18]. Mature SREBPs then bind to the sterol regulatory element (SRE) or the E-box sequences on the promoters of their target genes involved in fatty acid and cholesterol biosynthesis[19]. Therefore, small molecule inhibition of SREBPs may be an effective strategy for the treatment of metabolic diseases such as obesity, T2D, and atherosclerosis[20].

Heat shock protein 90 (HSP90), a member of the molecular chaperone family, plays a vital role in ensuring the proper folding of numerous newly created peptides and refolding denatured/misfolded client proteins. The involvement of HSP90 in metabolic disorders has been a focus of interest lately, yet the specific way in which HSP90 influences lipid metabolism is unclear. 17-AAG and Corylin have been shown to effectively reverse metabolic diseases by inhibiting HSP90 activity[21-23].

While HSP90β inhibitors like Corylin are known to regulate SREBP activity, endogenous modulators of this pathway remain unexplored. Bilirubin, a natural antioxidant with metabolic benefits, shares structural similarities with HSP90 ligands. Here, we demonstrate that bilirubin selectively targets HSP90β to suppress SREBP activation - a mechanism distinct from its known functions. Our findings reveal bilirubin as the first endogenous HSP90β-specific regulator of lipid metabolism, providing new insights into physiological metabolic control and therapeutic development.

METHODS

Reagents

Reagents and antibodies were procured from commercial sources as follows: Bilirubin was obtained from Shanghai Yousi De Biotech Co., Ltd (Shanghai, China). Luciferase assay kits were sourced from Promega Corporation (Madison, WI, USA). 3-(4,5-Dimethylthiazol-2-yl)-2,5-diphenyltetrazolium bromide (MTT), 25-hydroxycholesterol (25-HC), lovastatin, and compactin were purchased from Sigma-Aldrich (St. Louis, MO, USA). Cell culture components including fetal bovine serum (FBS), Dulbecco's Modified Eagle Medium (DMEM), and F-12K Nutrient Mixture (Ham's) were acquired from Gibco Laboratories (Grand Island, NY, USA). Lipoprotein-deficient serum (LPDS) was procured from Kalen Biomedical (Montgomery Village, MD, USA). Primary antibodies used in this study included: anti-SREBP-1 (mouse monoclonal, catalog #sc-8984; Santa Cruz Biotechnology, Dallas, TX, USA), anti-β-actin (mouse monoclonal, catalog #sc-47778; Santa Cruz Biotechnology), and anti-SREBP-2 (rabbit polyclonal, catalog #ab30682; Abcam, Cambridge, UK).

Cell culture

The human hepatocyte cell line HL-7702 was procured from Keygen Biotech (Nanjing, China). All cell cultures were maintained under standard conditions (37 °C, 5% CO_2) in DMEM supplemented with 10% FBS. To generate the HL-7702/SRE-Luc reporter cell line, HL-7702 cells were transfected with the pSRE-Luc plasmid, followed by monoclonal selection in hygromycin B-supplemented medium (Roche, Germany).

Cell proliferation assay

Cell growth was assessed using the MTT assays. HL-7702 cells were placed in 96-well dishes at a density of 2.0×10^4 cells per well in DMEM supplemented with 10% FBS for 24 h. Subsequently, the cells were exposed to varying concentrations of Bilirubin (12.5, 25, 50, 100, 200, 400 μM) or vehicle control (0.1% DMSO) for 18 h. Then, MTT solution (5 mg/mL in PBS) was added to each well (10 μL/well) and incubated for 4 h at 37 °C. The supernatant was then removed, and 150 μL of DMSO was introduced to each well to dissolve the formazan crystals. The absorbance was measured at 570 nm with a reference wavelength of 630 nm using a microplate reader (BioTek Synergy H1). Six biological replicates were performed for each condition, and

data were normalized to the untreated control group.

Luciferase reporter assay

HL-7702/SRE-Luc cells were placed in a 96-well plate, exposed to Bilirubin or untreated, and grown in DMEM with 5% lipoprotein-deficient FBS, 10 μM compactin, and 10 μM mevalonate (Medium E) for 18 h. Then, the medium was discarded. After being washed twice in PBS, the cells were then incubated in reporter lysis buffer at room temperature for 20 min. Afterward, the fluid was moved to the 96-well white dish, and the solution for the luciferase test was poured into each well while in darkness. Luminescence was immediately measured using a GloMax Navigator microplate luminometer (Promega). Firefly luciferase activity was normalized to total protein concentration determined by BCA assay.

Western blot analysis

After being rinsed with cold PBS, HL-7702 cells were then treated with RIPA buffer containing 50 mM Tris-HCl, pH 8.0, 150 mM NaCl, 1% Nonidet P-40, 0.5% sodium deoxycholate, 0.1% SDS, 1 mM EDTA, and protease inhibitors. Cell lysates were incubated on ice for 30 min with intermittent vortexing to ensure complete lysis. The lysates were then centrifuged to remove cellular debris. For sample preparation, protein extracts were mixed with 5 × SDS loading buffer (250 mM Tris-HCl pH 6.8, 10% SDS, 30% glycerol, 5% β-mercaptoethanol, 0.02% bromophenol blue) at a 4:1 ratio (v/v). The samples were heated at 100 °C for 10 min in a heating block to denature proteins. Cellular extracts were subjected to SDS-PAGE separation and then transferred onto PVDF membranes. 5% skim milk in PBS with 0.1% Tween-20 (PBST) was used to block the membranes. Next, antibodies against SREBP1 (Santa Cruz, USA), SREBP2 (Abcam, USA), and Actin (Beyotime Biotechnology, China) were incubated overnight at 4 °C. Following the three times PBST wash (5 min per wash), the HRP-conjugated secondary antibody from Beyotime Biotechnology in China was incubated for 1 h at ambient temperature. Following secondary antibody incubation, membranes were washed three times with PBST (5 min per wash) to ensure complete removal of unbound secondary antibodies. Chemi-Lumi One Ultra (Tanon, China) was used to detect immunoreactive signals.

Quantitative real-time PCR

RNA was extracted using Trizol (Vazyme, Nanjing, China) following the provided guidelines. RNA levels were standardized and transformed into cDNA with the help of Hiscript II reverse transcriptase from Vazyme in Nanjing, China. The LightCycler 96 Real-Time PCR System from Roche in Basel, Switzerland, was utilized to quantify gene expression with SYBR-green dyes. The analysis of all data was conducted with the GAPDH gene expression serving as the internal standard. Table 1 contains a list of the primers' sequences utilized.

Animal experiments

Association for Assessment and Accreditation of Laboratory Animal Care International has accredited the animal experimental center. Animals received human care following the National Institutes of Health's Guide to the Care and Use of Laboratory Animals. All animal experiments and care were approved by the Animal Ethics Committee of China Pharmaceutical University (2024-06-017). Every mouse was kept in communal cages and kept on a schedule of light and darkness. Every mouse was given either a high-fat diet (HFD) (TROPHIC, Nantong, China) or a standard diet (TROPHIC, Nantong, China). The HFD (product#; TP23300) had 60% fat, 20.6% carbs, and 19.4% protein per calorie, while the regular diet (product#; XT007) had 13% fat, 60% carbs, and 27% protein. Male C57BL/6J mice (6 weeks old) from Nanjing Biomedical Research Institute were acclimated for 1 week and randomly divided into four groups (n = 12): Chow + vehicle, HFD + vehicle, HFD + lovastatin (30 mg/kg/day orally in 0.5% CMC-Na), and HFD + bilirubin (20 mg/kg/day i.p.). Treatments continued for 6 weeks with respective diets. After overnight fasting, mice were euthanized by cervical dislocation following approved guidelines.

Table 1. Primers used for qPCR

Specifies	Gene name	Sequence of forward and reverse primers (5′ to 3′)
Homo sapiens	*SREBP-1c*	TCACAGTGACTGAGCTTCAGCA TCATCTTCATCACACCCAGGAC
	ACC1	ATGTCTGGCTTGCACCTAGTA CCCCAAAGCGAGTAACAAATTCT
	SCD	ATGTCTGGCTTGCACCTAGTA CCCCAAAGCGAGTAACAAATTCT
	FASN	CCGAGACACTCGTGGGCTA CTTCAGCAGGACATTGATGCC
	FASD2	ATGTCTGGCTTGCACCTAGTA CCCCAAAGCGAGTAACAAATTCT
	SCD2	CTCTGCGAGTGAATTTGGC GATCATCGGCTTGGTTGC
	SREBP-2	TCACAGTGACTGAGCTTCAGCA TCATCTTCATCACACCCAGGAC
	HMGCR	TCACAGTGACTGAGCTTCAGCA TCATCTTCATCACACCCAGGAC
	LDLR	TCACAGTGACTGAGCTTCAGCA TCATCTTCATCACACCCAGGAC
	HMGCS1	CTCTTGGGATGGACGGTATGC GCTCCAACTCCACCTGTAGG
	MVK	GGAGCAAGGTGATGTCACAAC CGGCAGATGGACAGGTATAAGT
	FPPS	TGTGACCGGCAAAATTGGC GCCCGTTGCAGACACTGAA
	FDFT1	CCACCCCGAAGAGTTCTACAA TGCGACTGGTCTGATTGAGATA
	LSS	GTACGAGCCCGGAACATTCTT CGGCGTAGCAGTAGCTCAT
	INSIG1	CCTGGCATCATCGCCTGTT AGAGTGACATTCCTCTGGATCTG
	SE	CCTCTTTGTCTTTACGGTTTCC GTCCCAGTGCCTTTGATGTT
	DHCR7	GCTGCAAAATCGCAACCCAA GCTCGCCAGTGAAAACCAGT
	MSMO1	TGCTTTGGTTGTGCAGTCATT GGATGTGCATATTCAGCTTCCA
	APOE	GTTGCTGGTCACATTCCTGG GCAGGTAATCCCAAAAGCGAC
	ACLY	ATCGGTTCAAGTATGCTCGGG GACCAAGTTTTCCACGACGTT
	PSCK9	GAGACCCAGAGGCTACAGATT AATGTACTCCACATGGGGCAA
Mus musculus	*GAPDH*	GGAGCGAGATCCCTCCAAAAT GGCTGTTGTCATACTTCTCATGG
	SREBP-1	ACAGTGACTTCCCTGGCCTAT GCATGGACGGGTACATCTTCAA
	FASN	GCTGCGGAAACTTCAGGAAAT AGAGACGTGTCACTCCTGGACTT
	SCD-1	GCTGCGGAAACTTCAGGAAAT AGAGACGTGTCACTCCTGGACTT
	ACS	GCTGCCGACGGGATCAG TCCAGACACATTGAGCATGTCAT
	ACC	GCTGCGGAAACTTCAGGAAAT AGAGACGTGTCACTCCTGGACTT
	ACL	GCTGCGGAAACTTCAGGAAAT AGAGACGTGTCACTCCTGGACTT
	FASD-1	CTACCCCGCGCTACTTCAC CGGTCGATCACTAGCCACC

FASD-2	GACCACGGCAAGAACTCAAAG GAGGGTAGGAATCCAGCCATT
SREBP-2	GCGTTCTGGAGACCATGGA ACAAAGTTGCTCTGAAAACAAATCA
HMGCS	GCGTTCTGGAGACCATGGA ACAAAGTTGCTCTGAAAACAAATCA
HMGCR	GCGTTCTGGAGACCATGGA ACAAAGTTGCTCTGAAAACAAATCA
LDLR	ATTTGCTCACCGTGGAGATGTT GAAGTCATCCAGGCCACTACTAATG
SCAP	ATTTGCTCACCGTGGAGATGTT GAAGTCATCCAGGCCACTACTAATG
FDPS	ATTTGCTCACCGTGGAGATGTT GAAGTCATCCAGGCCACTACTAATG
INSIG-1	TCACAGTGACTGAGCTTCAGCA TCATCTTCATCACACCCAGGAC
INSIG-2a	TCACAGTGACTGAGCTTCAGCA TCATCTTCATCACACCCAGGAC
INSIG-2b	TCACAGTGACTGAGCTTCAGCA TCATCTTCATCACACCCAGGAC

qPCR: Quantitative Real-time PCR.

Tests for glucose and insulin tolerance

For glucose tolerance tests (GTT), mice were fasted for 12-16 h (overnight) with water available, then administered 2 g/kg glucose (Sigma) by oral gavage. For insulin tolerance tests (ITT), mice were fasted for 4-6 h before receiving 0.75 U/kg insulin (Sigma) via intraperitoneal injection. In both tests, blood glucose levels were measured from tail vein samples at 0, 15, 30, 60, and 120 min post-administration using a glucometer (OneTouch Ultra). The area under the curve (AUC) was calculated for quantitative comparison. All animals were allowed to recover for 3 days after metabolic tests before tissue collection.

Measurement of lipids in the serum and liver

Serum lipid profile, including total cholesterol (TC), TG, low- and high-density lipoprotein cholesterol (LDL-C, HDL-C), along with hepatic function markers [alanine aminotransferase (ALT), aspartate aminotransferase (AST)], were assessed using commercial enzymatic assay kits (Nanjing Jiancheng Bioengineering Institute, China) on a Biotek automated analyzer (USA). Insulin levels were quantified via enzyme-linked immunosorbent assay (ELISA, CUSABIO, China). Additionally, intrahepatic cholesterol and TG content were quantified in liver tissue homogenates.

Histological analysis of liver and adipose tissues

Freshly dissected tissues [liver, interscapular brown adipose tissue (BAT), and epididymal white adipose tissue (WAT)] were immediately fixed in 4% paraformaldehyde (PFA) at 4 °C for 24 h. After fixation, samples were dehydrated, embedded in paraffin, and sectioned at 5 μm thickness using a rotary microtome. Sections were mounted on poly-L-lysine-coated slides and stained with hematoxylin and eosin (H&E) for histological evaluation. For lipid visualization, liver specimens were embedded in Tissue-Tek OCT compound (Leica Biosystems, China) and frozen at -20 °C. Cryosections (10 μm) were prepared using a cryostat (Leica CM1950) and stained with 0.5% Oil Red O solution (Sigma-Aldrich, USA) to assess neutral lipid accumulation.

Virtual docking assay

The HSP90β crystal structures (3PRY) were obtained from the RCSB protein data bank for use in molecular docking. The water molecules in the crystal structure of 3PRY were eliminated. Maestro sketched the compound, which was then processed by LigPrep using its default parameters. Molecular docking was performed using Glide (Schrödinger, LLC, New York, NY, USA) in XP mode.

Microscale thermophoresis analysis

Bilirubin was titrated in HSP90β. The recombinant human HSP90β protein was expressed in Escherichia coli BL21 (DE3) as a C-terminal His6-tagged fusion protein using the pET28a expression system (Novagen) and purified via Ni^{2+}-affinity chromatography. The experiment took place in a solution containing 50 mM HEPES. Afterward, the samples were left to incubate at ambient temperature for 5 min before analysis using microscale thermophoresis. Thermophoresis measurements were conducted using a NanoTemper Monolith Instrument (NT.115). In this instrument, an infra blue Laser (IB-Laser) beam couples into the path of light with a dichroic mirror and is focused into the sample fluid through the same optical element used for fluorescence imaging. For the analysis of the thermophoresis of a sample, 10 mL of the sample was moved into a glass capillary that had been treated to be hydrophilic (NanoTemper). The protein's thermophoresis was studied with different levels of the compound for 30 s. The tests were conducted at room temperature, and the standard deviation (SD) was determined based on three separate trials.

Statistical analysis

For comparisons across multiple groups (e.g., Chow, HFD, Lovastatin, Bilirubin), we have used one-way ANOVA followed by Tukey's post-hoc test to account for multiple comparisons. For time-course data (e.g., GTT, ITT), we have applied two-way ANOVA with Bonferroni correction to evaluate both group and time effects. Other experimental results are expressed as mean ± SD. Intergroup comparisons were performed using two-tailed Student's *t*-tests. A P value < 0.05 was considered statistically significant.

RESULTS

Bilirubin reduces lipid accumulation in hepatocytes induced by PA/OA

We first investigated the effect of bilirubin on reducing lipid accumulation in hepatocytes. Human HL-7702 normal liver cells were treated with bilirubin [Figure 1A] (5, 10, and 20 μM) in the presence of palmitic acid (PA) and oleic acid (OA) for 16 h. Quantitative assessment of intracellular TG and TC levels validated bilirubin's efficacy in reducing lipid accumulation. [Figure 1B and C], without significant cytotoxicity [Figure 1D]. Fluorescent staining with Nile Red, a neutral lipid-specific dye, revealed that bilirubin treatment markedly reduced both the quantity and diameter of intracellular lipid droplets in hepatocytes [Figure 1E]. These data indicate that bilirubin reduces lipid accumulation induced by PA/OA in hepatocytes.

Bilirubin attenuates ectopic lipid deposition in hepatic and adipose tissues of DIO mice

To confirm the ability of bilirubin to reduce lipids in living organisms, C57BL/6J mice fed a HFD were given either a vehicle (0.5% CMC-Na), lovastatin (30 mg/kg/day), or bilirubin (20 mg/kg/day) for 6 weeks [Figure 2A]. There was no notable variation in the amount of food intake by any of the groups [Figure 2B]. Bilirubin hindered the rise in body weight [Figure 2C] induced by HFD. To further elucidate the therapeutic effects of bilirubin on lipid metabolism in DIO mice, the lipid levels in the blood and liver were measured. Following a 6-week treatment regimen with bilirubin (20 mg/kg), biochemical analyses revealed a significant reduction in serum TC, TG, and LDL-C [Figure 2D-F], alongside a pronounced elevation in HDL-C levels [Figure 2G]. Furthermore, bilirubin and lovastatin both reduced liver weight [Figure 2H] and inhibited hepatic TC and TG accumulation in the liver of mice [Figure 2I and J]. Accumulation of fat in the liver leads to liver damage, as shown by elevated levels of ALT and AST in the blood. Like lovastatin, bilirubin markedly reduced the level of serum AST and ALT in DIO mice [Figure 2K and L]. In line with the lipid level data, histological examination revealed that bilirubin notably decreased the buildup of lipid droplets in the livers of DIO mice compared to those fed a regular diet, like lovastatin [Figure 2M]. The findings indicated that, unlike lovastatin, bilirubin hinders the buildup of lipids in the livers of DIO mice.

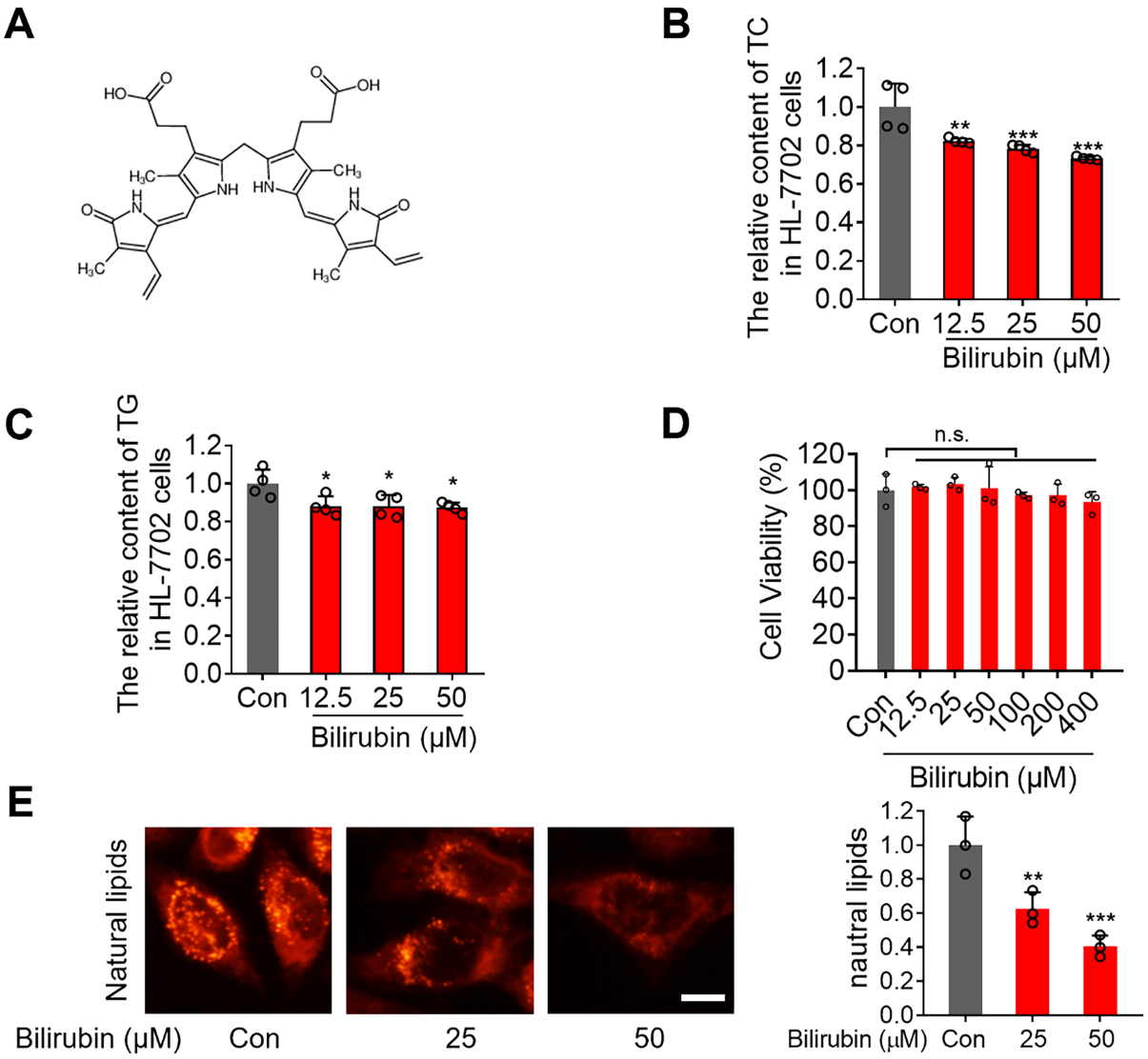

Figure 1. Bilirubin inhibits intracellular lipid accumulation *in vitro*. (A) Chemical structure of bilirubin; (B and C) Cellular TC (B) and TG (C) contents measured in human liver HL-7702 cells treated with DMSO or Bilirubin (12.5, 25, 50 μM) for 24 h; (D) Cell viability of HL-7702 cells treated with increasing concentrations of bilirubin (12.5-400 μM) for 24 h, assessed by MTT assay; (E) Following fixation, cells were stained with Nile Red to visualize neutral lipids. Quantification of lipid droplets was performed using IPP software based on three independent experiments. Scale bar = 10 μm. IPP: Image-Pro plus; MTT: 3-(4,5-Dimethylthiazol-2-yl)-2,5-diphenyltetrazolium bromide; TC: total cholesterol; TG: triglyceride. $^{*}P < 0.05$; $^{**}P < 0.01$; $^{***}P < 0.001$ *vs.* Con.

Bilirubin at a dosage of 20 mg/kg significantly decreased the size of adipocytes in DIO mice within WAT [Figure 2M]. Furthermore, bilirubin and lovastatin both decreased the dimensions of BAT [Figure 2M]. Overall, the findings indicated that bilirubin improves lipid storage in the liver and adipose tissues of DIO mice.

Bilirubin ameliorates glucose homeostasis and insulin resistance in DIO mice

Given that bilirubin hindered the buildup of lipids in both the bloodstream and tissues, our subsequent investigation focused on determining if bilirubin improved glucose regulation and insulin resistance. The mice fed a HFD showed worse glucose tolerance and resistance to insulin compared to mice fed a regular diet. Remarkably, the high fasting blood glucose and insulin levels were significantly improved in bilirubin-

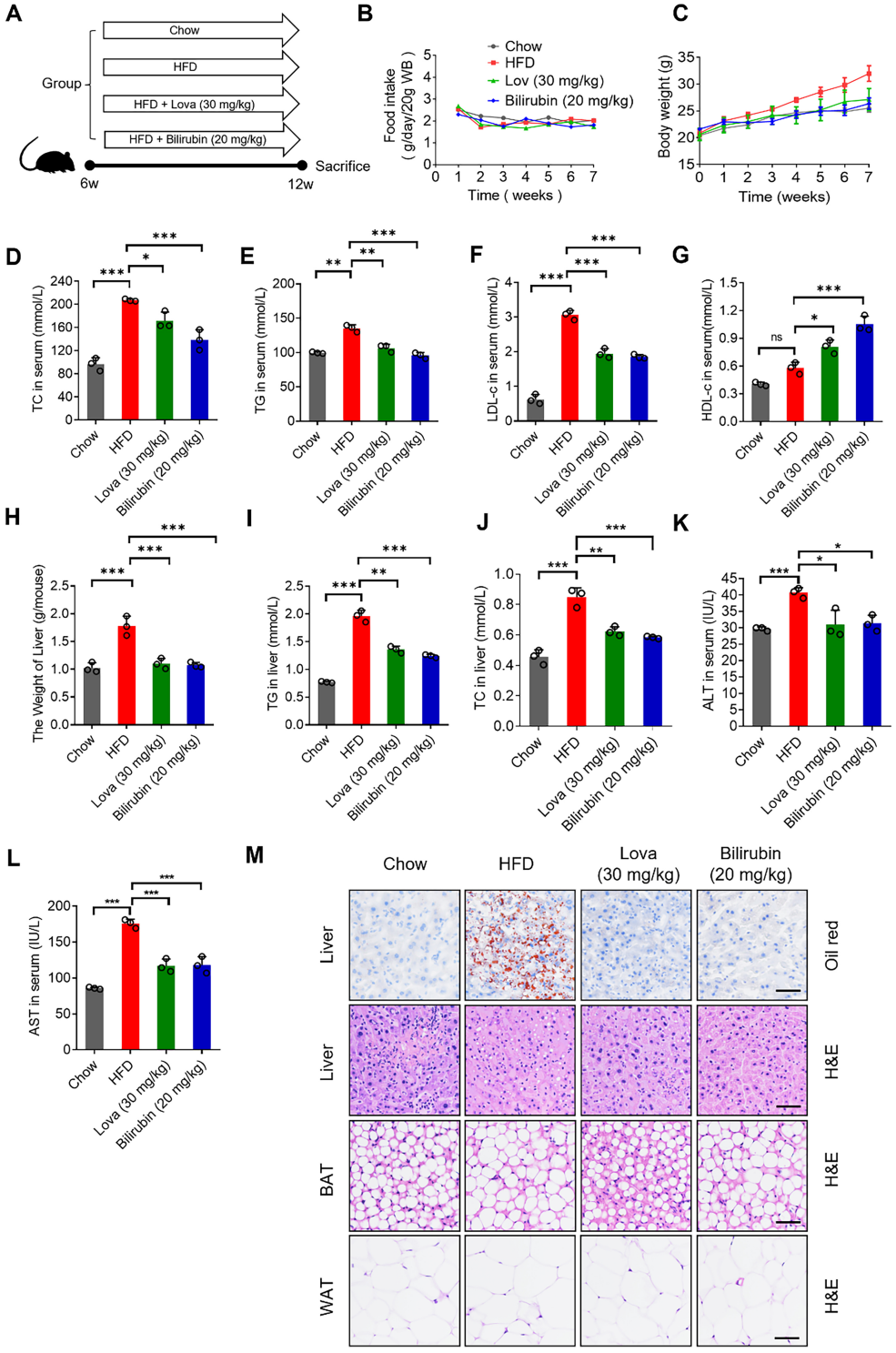

Figure 2. Bilirubin reduces lipid levels in HFD-fed mice. (A) Experimental design for each group in the HFD mouse model; (B and C) Food intake and body weight; (D-G) Effects of bilirubin on blood TG, TC, LDL-C, and HDL-C levels; (H) Liver weight (g/mouse); (I and J) Effects of bilirubin on hepatic TG and TC levels; (K and L) Effects of bilirubin on serum ALT and AST levels; (M) Macroscopic evaluation of hepatic morphology, along with histopathological examination of the liver, WAT, and BAT. Scale bar = 50 μm. $n = 3$. HFD: High-fat diet; TC: total cholesterol; TG: triglyceride; LDL-C: low-density lipoprotein cholesterol; HDL-C: high-density lipoprotein cholesterol; ALT: alanine aminotransferase; AST: aspartate aminotransferase; WAT: white adipose tissue. $^{*}P < 0.05$; $^{**}P < 0.01$; $^{***}P < 0.001$ *vs.* HFD.

treated mice on a HFD [Figure 3A and B]. Additionally, bilirubin administration effectively restored impaired glucose homeostasis and mitigated insulin insensitivity in DIO murine models. [Figure 3C-F]. Collectively, these findings demonstrate bilirubin's efficacy in enhancing glycemic control and alleviating insulin resistance.

Bilirubin improves lipid accumulation by regulating the SREBP pathway *in vitro*

Bilirubin reduced intracellular cholesterol and TG levels [Figure 1A-C] in human hepatocytes HL-7702 cells. Bilirubin was found to have an inhibitory effect on cholesterol and TG accumulation *in vitro* when compared to the vehicle control. SREBPs play a significant role in controlling the activation of genes related to the production of cholesterol, fatty acids, and TG. As expected, 25-HC, a canonical SREBP suppressor, markedly attenuated luciferase reporter activity in positive control assays. This indicates that the SRE-Luc reporter system is functioning correctly. Based on these observations, we postulated that bilirubin-mediated attenuation of lipid deposition may result from its regulatory effects on SREBP transcriptional activity. Bilirubin was identified as an inhibitor of SREBP by utilizing a human hepatocyte cell line, HL-7702, which contained a luciferase expression cassette driven by SRE. As shown in Figure 4A and B, bilirubin effectively suppressed SREBP function in a manner that depended on both concentration and time. In line with the findings of SREBP transactivation, bilirubin significantly reduced the levels of both mature SREBP-1 and SREBP-2 in HL-7702 cells [Figure 4C-F]. Gene expression analysis via qPCR in HL-7702 hepatocytes demonstrated that bilirubin markedly suppressed the transcriptional activity of SREBP-1, as evidenced by downregulation of key lipogenic enzymes such as fatty acid synthase (FAS), acetyl-CoA carboxylase 1 (ACC1), and stearoyl-CoA desaturase-1 (SCD-1) [Figure 4G]. Fifteen genes related to cholesterol synthesis, including *SREBP-2, HMGCR, HMGCS, LSS, FDPS, MVK,* and *FDFT1*, are regulated by SREBP-2 [Figure 4H]. The data above indicate that bilirubin may reduce cholesterol and TG buildup *in vitro* by inhibiting SREBP processing.

Bilirubin improves lipid accumulation by regulating the SREBP pathway *in vivo*

To investigate the role of SREBPs in the effects of bilirubin on DIO mice, hepatic SREBP levels were examined in each mouse group. As shown in Figure 5A and B, bilirubin treatment notably reduced the hepatic protein level of SREBP-1 in DIO mice. Next, we assessed the expression of SREBP target genes and other associated genes in the livers of these mice. Quantitative PCR analysis demonstrated that bilirubin treatment significantly downregulated hepatic expression of both SREBP-1 and SREBP-2 transcripts in DIO mice [Figure 5C and D]. Bilirubin treatment markedly suppressed hepatic expression of SREBP-1-dependent lipogenic genes, particularly *FASN, SCD-1, ACS, ACC, ACL,* and *FASD-2* in DIO mice [Figure 5C]. Likewise, bilirubin treatment markedly reduced hepatic expression of SREBP-2-regulated genes (*HMGCS, HMGCR, LDLR, FDPS*) critical for cholesterol synthesis in DIO mice [Figure 5D]. Collectively, our findings suggest that bilirubin-controlled SREBPs affect genes related to metabolism and lipid accumulation in liver and adipose tissues, potentially improving insulin sensitivity.

Bilirubin is a specific inhibitor of HSP90β

The significance of HSP90 in metabolic disorders has recently become a focal point. Studies have shown that blocking HSP90 with 17-AAG and corylin can effectively reverse metabolic diseases. Given these findings, we hypothesized that bilirubin could potentially inhibit SREBP activation by suppressing HSP90. To confirm this hypothesis, we initially examined if bilirubin interacts with HSP90 using a computerized docking test. The findings indicated that the affinity between HSP90 and bilirubin is -6.86 kJ/mol, as illustrated in Figure 6A. Subsequently, we discovered a sole possible binding site situated between amino acids 312 and 439 in the molecular dynamics of HSP90β with the assistance of Maestro [Figure 6A], a distinct pocket separates from HSP90α. Molecular interaction analysis revealed five hydrogen bonds linking HSP90β residues (TRP-312, ARH-338, ALA-339, PRO-340, ARG-378) with bilirubin, identified via

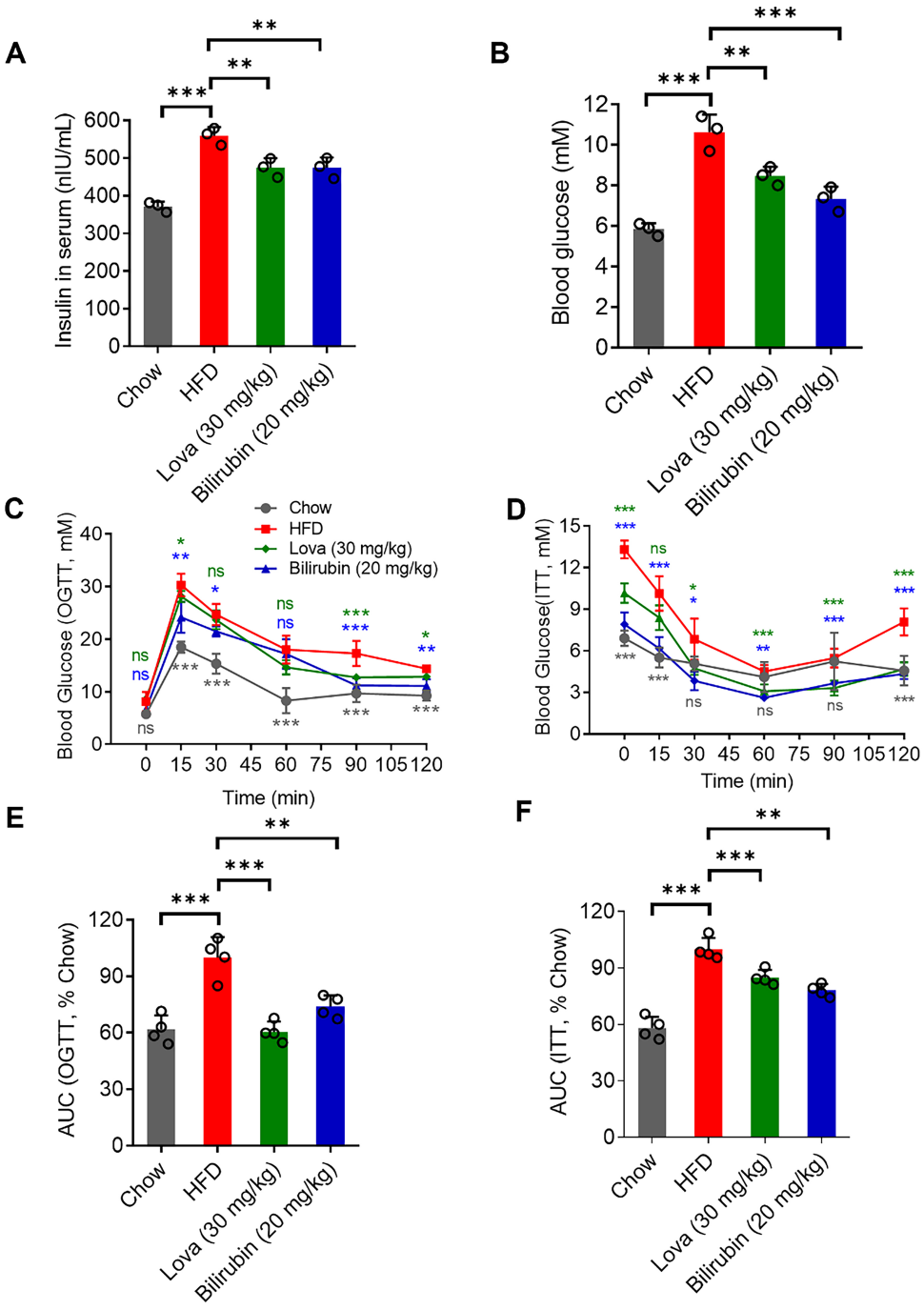

Figure 3. Bilirubin administration ameliorates glucose tolerance and enhances insulin sensitivity in HFD-fed mice. (A and B) Bilirubin administration significantly decreased blood insulin levels (A) and blood glucose levels (B) in HFD-fed mice; (C) Effects of bilirubin on glucose homeostasis in high-fat diet-induced obese mice, as assessed by OGTT; (D) Effects of bilirubin on insulin resistance in HFD-fed mice, as determined by ITT; (E) Quantitative analysis of the AUC for OGTT in (C); (F) Quantitative analysis of the AUC for ITT in (D). HFD: High-fat diet; OGTT: oral glucose tolerance test; ITT: insulin tolerance test; AUC: area under the curve. $^{*}P < 0.05$; $^{**}P < 0.01$; $^{***}P < 0.001$ *vs.* HFD.

structural mapping and sequence alignment [Figure 6A]. Following this, the MST assay revealed a clear connection between bilirubin and HSP90, indicating a KD of 233.23 ± 305.97 nM [Figure 6B]. These results demonstrated that bilirubin targets HSP90β and inhibits SREBP activity.

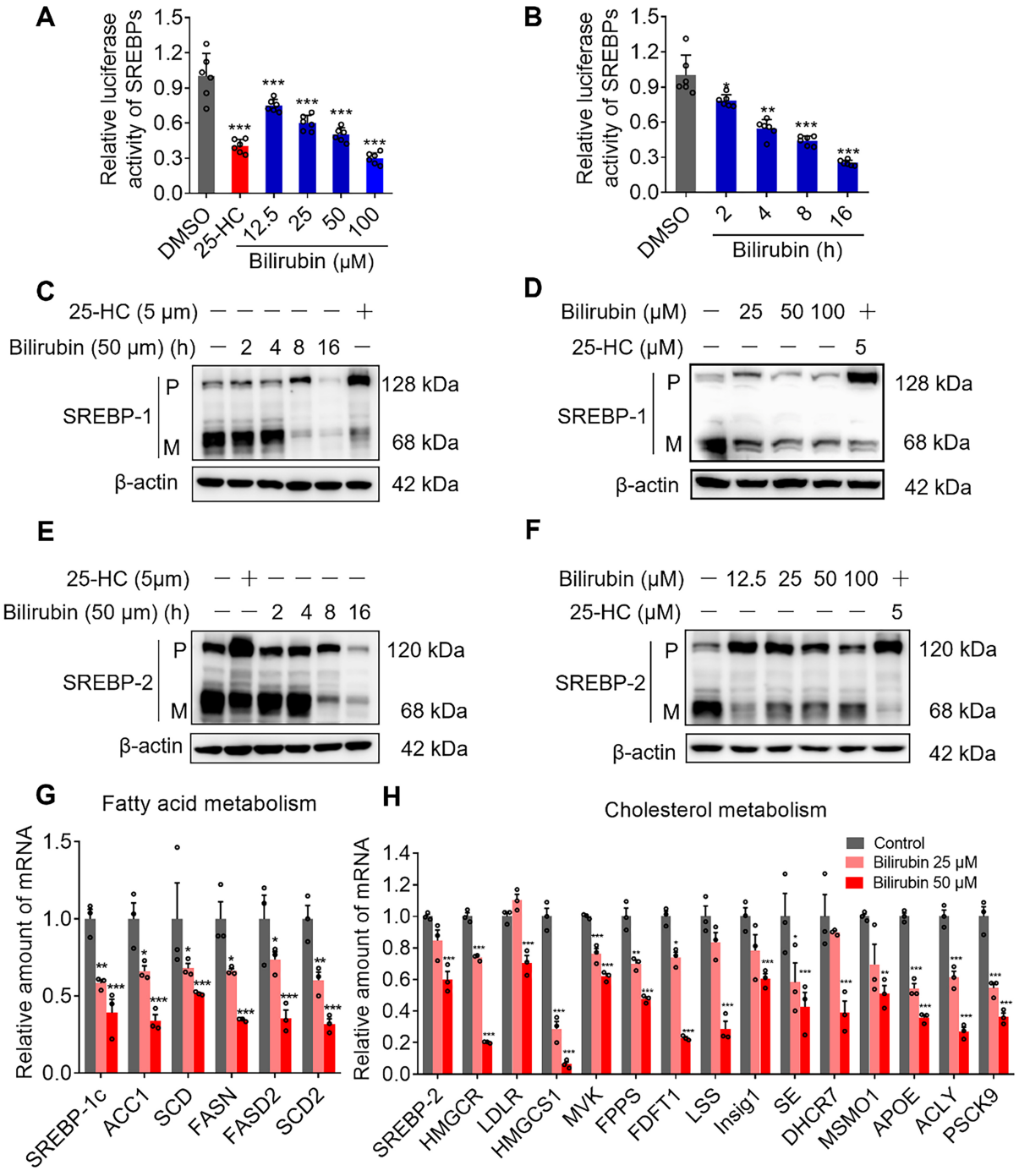

Figure 4. Bilirubin inhibits SREBP activity *in vitro*. (A) SRE-Luc/HL-7702 cells were treated with bilirubin (12.5-100 μM) for 6 h before cell lysis and luciferase activity measurement; (B) Time-course analysis of SRE-Luc reporter activity in HL-7,702 cells treated with bilirubin (50 μM) for 2-16 h; (C-F) Immunoblot analysis of HL-7702 whole-cell lysates using specific antibodies; (G and H) Q-PCR analysis of gene expression changes in HL-7702 cells following bilirubin treatment (25/50 μM). All experiments were performed in biological triplicates. SREBP: Sterol regulatory element-binding proteins; SRE: sterol regulatory element.

DISCUSSION

Bilirubin, a heme catabolite, has traditionally been associated with jaundice and liver dysfunction[24]. However, recent research has revealed that bilirubin is not just a metabolic waste product but also a

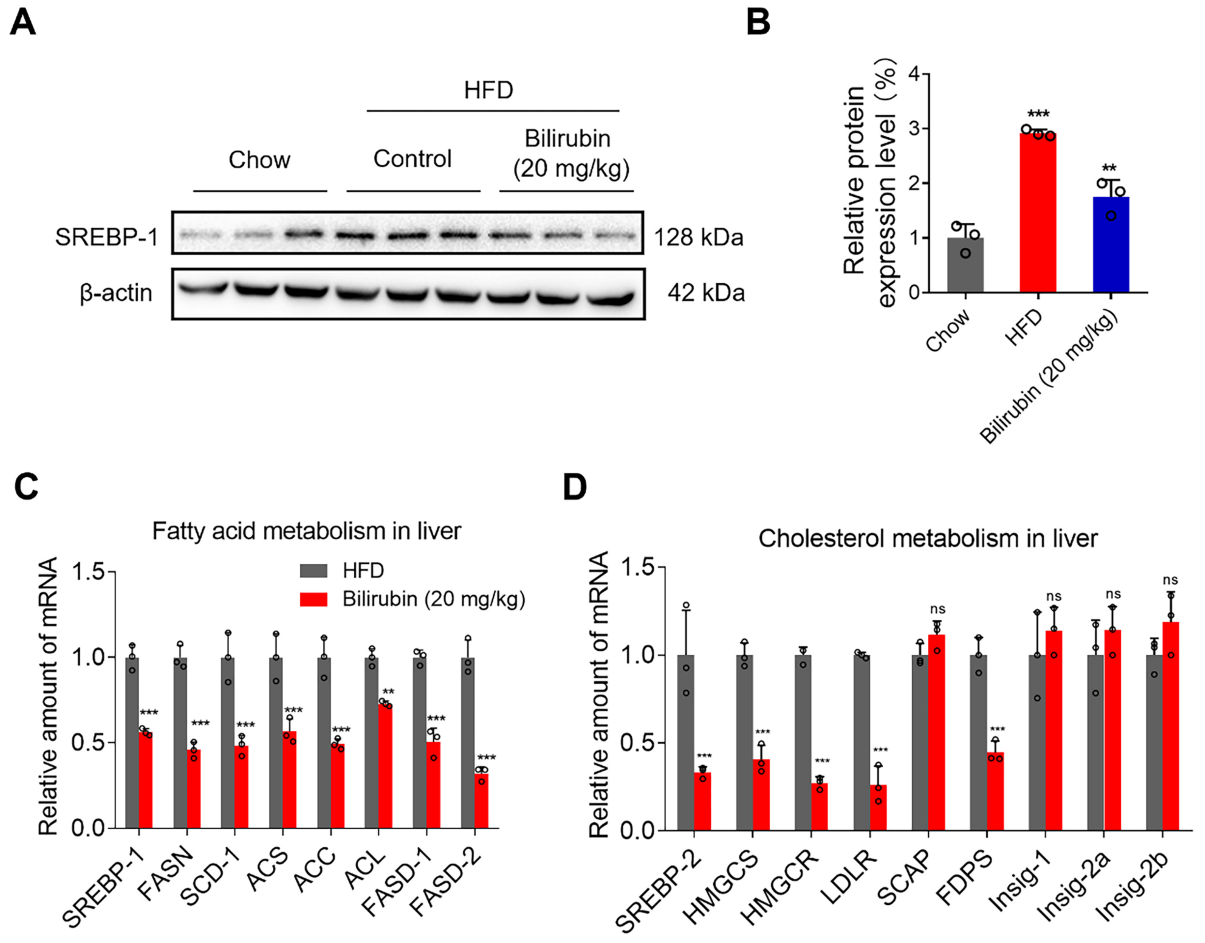

Figure 5. Bilirubin inhibits the SREBP activity in HFD-fed mice. (A) Liver protein lysates (pooled from 3 mice/group) were immunoblotted with target-specific antibodies; (B) SREBP-1 expression levels were normalized to GAPDH for quantitative analysis; (C and D) Hepatic RNA extracts underwent Q-PCR quantification using mouse GAPDH as an endogenous control, per established protocols. Error bars represent standard deviations. $n = 3$. $^{*}P < 0.05$; $^{**}P < 0.01$; $^{***}P < 0.001$ *vs.* HFD. SREBP: Sterol regulatory element-binding proteins; HFD: high-fat diet.

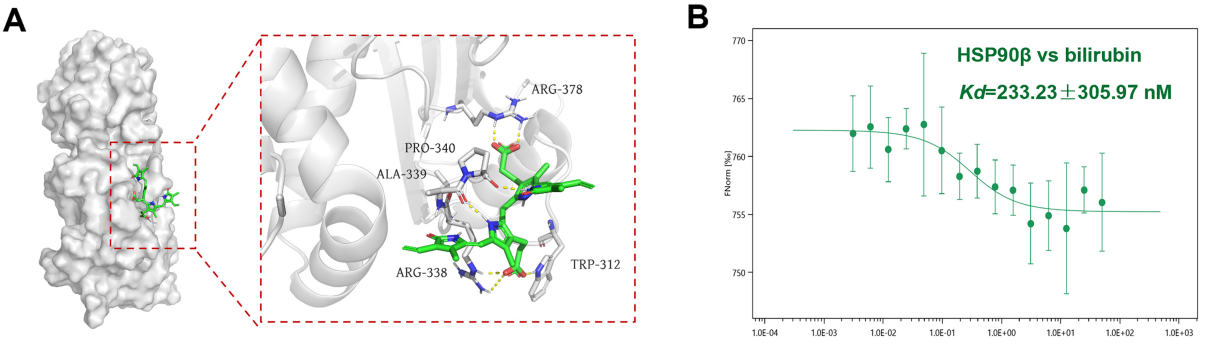

Figure 6. Bilirubin binds specifically to HSP90β. (A) Computational docking analysis (PDB: 3PRY) revealed that bilirubin localizes within the middle domain of HSP90β (residues 312-439), forming hydrogen bonds with TRP-312, ARH-338, ALA-339, PRO-340, and ARG-378; (B) MST assays confirmed the direct binding interaction between bilirubin and HSP90β.

bioactive molecule capable of modulating multiple signaling pathways[25]. Bilirubin exerts anti-inflammatory effects by inhibiting NF-κB signaling[26], reduces oxidative stress via ROS scavenging[27], and modulates

nuclear receptors (e.g., AhR) to regulate immunity and metabolism[28]. It also suppresses apoptosis, promoting cell survival[29], highlighting its multifaceted protective roles in disease prevention. Low serum bilirubin levels correlate with increased risks of obesity, metabolic syndrome, and T2D. Bilirubin activates PPAR-α, promoting brown fat and reducing white fat accumulation. Higher bilirubin may also mitigate diabetic complications. Modulating bilirubin levels could offer therapeutic potential for metabolic disorders[30].

Animal studies demonstrate bilirubin's therapeutic effects at concentrations of 0.5-200 μM, though optimal doses vary by model[31]. *In vitro* and organ studies (e.g., kidney/liver) show efficacy at 5-20 μM, with toxicity above 25 μM[32]. Systemic delivery *in vivo* requires higher doses (e.g., 148 μM in cholestatic rats) due to physiological buffering (protein binding, excretion)[33]. Gunn rat models revealed dose-dependent protection (6.8 μM partial, 71 μM complete). Parenteral bilirubin (3-20 mg/kg) mitigated ischemia-reperfusion injury (e.g., 220 μM reduced intestinal damage) but failed to preserve renal function. Clinical translation remains limited by formulation challenges. Current bilirubin preparations, primarily animal-derived (e.g., porcine isomers), pose prion/viral risks and are unsuitable for human use[28]. Its poor water solubility (requiring pH > 9.5 or DMSO) and high plasma protein binding limit bioavailability, necessitating frequent dosing.

While this study demonstrates bilirubin's therapeutic potential in metabolic disorders, several limitations should be noted. First, the animal model may not fully replicate human metabolic syndrome pathophysiology. Second, the precise molecular mechanisms by which bilirubin modulates the HSP90β/SREBP axis remain incompletely characterized, particularly regarding potential crosstalk with other metabolic pathways. Third, the potential off-target effects of bilirubin were not comprehensively evaluated. Finally, the translational relevance of dosing regimens (20 mg/kg in mice) to human applications warrants additional pharmacokinetic studies. Future investigations should employ proteomic and metabolomic approaches to further elucidate the mechanistic underpinnings and optimize therapeutic strategies for clinical translation.

Our study demonstrates bilirubin's novel role in improving HFD-induced metabolic disorders through inhibition of HSP90β to suppress SREBP activation. Building on our previous work establishing HSP90β-SREBP regulation, we show bilirubin acts as an endogenous modulator of this pathway at physiologically relevant concentrations. Key findings reveal bilirubin's distinct advantages: (1) selective HSP9β targeting compared to pan-inhibitors like 17-AAG, potentially reducing toxicity; (2) dual benefits combining metabolic regulation with known antioxidant effects. The positive control lovastatin confirmed our model's validity while highlighting mechanistic differences - bilirubin modulates SREBP stability whereas statins directly inhibit cholesterol synthesis. Study limitations include the focus on hepatic effects and lack of bilirubin-treated Chow controls, which future work should address through: (1) systemic metabolic profiling; (2) structural studies of bilirubin-HSP90β binding; (3) expanded treatment groups. Nevertheless, our results establish bilirubin's therapeutic potential and reveal new aspects of endogenous metabolic regulation through the HSP90β-SREBP axis.

DECLARATIONS

Authors' contributions

Writing-original draft, writing-review and editing, methodology, formal analysis, investigation, resources, data curation: Zhu J

Writing-original draft, writing-review and editing, methodology, formal analysis, investigation, visualization: Xiao HT

Writing-original draft, investigation, data curation, validation: Wu QY
Investigation: Shao XX, Meng YF, He JX, Lai LN
Investigation, writing-original draft: Ding JX
Writing-review and editing, conceptualization, resources, supervision, project administration: Xue N
Writing-review and editing, conceptualization, resources, data curation, supervision, project administration, funding acquisition, conceptualization: Zheng ZG

Availability of data and materials

The original contributions presented in this study are included in thhe article. Further inquiries can be directedto the corresponding authors.

Financial support and sponsorship

This work was supported by the Jiangsu Provincial Traditional Chinese Medicine Science and Technology Development Plan (QN202426), Jiangsu Province "333 High-level Talents Training Project"[(2024)3-0189], Youth Talent Support Project of the Jiangsu Association for Science and Technology (TJ-2023-053), Shanxi Provincial Department-Municipal Key Laboratory Cultivation Base for Quality Enhancement and Utilization of Shangdang Chinese Medicinal Materials (KF202401), Fundamental Research Program of Shanxi Province (202403021221211), the Research Project Supported by the Shanxi Scholarship Council of China (No.2023-158), Hangzhou bio-medicine and health industry development support science and technology project (2024WJC104), and National Innovation and Entrepreneurship Training Program for Undergraduate(S202510316112).

Conflicts of interest

All authors declared that there are no conflicts of interest.

Ethical approval and consent to participate

All animal experiments and care were approved by the Animal Ethics Committee of China Pharmaceutical University (2024-06-017). The human hepatocyte cell line HL-7702 was procured from Keygen Biotech (Nanjing, China).

Consent for publication

Not applicable.

Copyright

© The Author(s) 2025.

REFERENCES

1. Alembagheri A, Hajimehdipoor H, Choopani R, Esmaeili S. The role of selected medicinal plants from Iranian traditional medicine for the treatment of fatigue in metabolic syndrome. *Tradit Med Res.* 2023;8:23. DOI
2. Kalisz K, Navin PJ, Itani M, Agarwal AK, Venkatesh SK, Rajiah PS. Multimodality imaging in metabolic syndrome: state-of-the-art review. *Radiographics.* 2024;44:e230083. DOI PubMed
3. Davids SF, Matsha TE, Peer N, Erasmus RT, Kengne AP. Changes in obesity phenotype distribution in mixed-ancestry South Africans in cape town between 2008/09 and 2014/16. *Front Endocrinol.* 2019;10:753. DOI PubMed PMC
4. Shen S, Liao Q, Gu L, et al. G protein-coupled receptor-biased signaling: potential drug discovery to facilitate treatment of metabolic diseases. *Acta Materia Medica.* 2024;3:31-45. DOI
5. Schmid A, Karrasch T, Schäffler A. The emerging role of bile acids in white adipose tissue. *Trends Endocrinol Metab.* 2023;34:718-34. DOI PubMed
6. Gálvez I, Navarro MC, Martín-Cordero L, Otero E, Hinchado MD, Ortega E. The influence of obesity and weight loss on the bioregulation of innate/inflammatory responses: macrophages and immunometabolism. *Nutrients.* 2022;14:612. DOI PubMed PMC
7. Fu M, Bao T, Yu H, et al. Metabolomics investigation on antiobesity effects of *Corydalis bungeana* on high-fat high-sugar diet-induced obese rats. *Chin Herb Med.* 2022;14:414-21. DOI PubMed PMC

8. Hugelshofer M, Buzzi RM, Schaer CA, et al. Haptoglobin administration into the subarachnoid space prevents hemoglobin-induced cerebral vasospasm. *J Clin Invest.* 2019;129:5219-35. DOI PubMed PMC
9. Walter ERH, Ge Y, Mason JC, Boyle JJ, Long NJ. A coumarin-porphyrin FRET break-apart probe for heme oxygenase-1. *J Am Chem Soc.* 2021;143:6460-9. DOI PubMed PMC
10. Vuerich M, Wang N, Graham JJ, et al. Blockade of PGK1 and ALDOA enhances bilirubin control of Th17 cells in Crohn's disease. *Commun Biol.* 2022;5:994. DOI PubMed PMC
11. Creeden JF, Gordon DM, Stec DE, Hinds TD Jr. Bilirubin as a metabolic hormone: the physiological relevance of low levels. *Am J Physiol Endocrinol Metab.* 2021;320:E191-207. DOI PubMed PMC
12. Wang S, Lin Y, Zhou Z, et al. Circadian clock gene bmal1 regulates bilirubin detoxification: a potential mechanism of feedback control of hyperbilirubinemia. *Theranostics.* 2019;9:5122-33. DOI PubMed PMC
13. Wang F, Chen S, Ren L, et al. The effect of silibinin on protein expression profile in white adipose tissue of obese mice. *Front Pharmacol.* 2020;11:55. DOI PubMed PMC
14. Chen W, Tumanov S, Fazakerley DJ, et al. Bilirubin deficiency renders mice susceptible to hepatic steatosis in the absence of insulin resistance. *Redox Biol.* 2021;47:102152. DOI PubMed PMC
15. Cheng C, Geng F, Li Z, et al. Ammonia stimulates SCAP/Insig dissociation and SREBP-1 activation to promote lipogenesis and tumour growth. *Nat Metab.* 2022;4:575-88. DOI PubMed PMC
16. Zhang C, Huang Z, Jing H, et al. SAK-HV triggered a short-period lipid-lowering biotherapy based on the energy model of liver proliferation via a novel pathway. *Theranostics.* 2017;7:1749-69. DOI PubMed PMC
17. DeBose-Boyd RA, Ye J. SREBPs in lipid metabolism, insulin signaling, and beyond. *Trends Biochem Sci.* 2018;43:358-68. DOI PubMed PMC
18. Podszun MC, Alawad AS, Lingala S, et al. Vitamin E treatment in NAFLD patients demonstrates that oxidative stress drives steatosis through upregulation of de-novo lipogenesis. *Redox Biol.* 2020;37:101710. DOI PubMed PMC
19. Shimano H, Sato R. SREBP-regulated lipid metabolism: convergent physiology - divergent pathophysiology. *Nat Rev Endocrinol.* 2017;13:710-30. DOI PubMed
20. Liu Y, Qiu N, Shen L, et al. Nanocarrier-mediated immunogenic chemotherapy for triple negative breast cancer. *J Control Release.* 2020;323:431-41. DOI PubMed PMC
21. Talaei S, Mellatyar H, Asadi A, Akbarzadeh A, Sheervalilou R, Zarghami N. Spotlight on 17-AAG as an Hsp90 inhibitor for molecular targeted cancer treatment. *Chem Biol Drug Des.* 2019;93:760-86. DOI PubMed
22. Zheng ZG, Zhang X, Liu XX, et al. Inhibition of HSP90β improves lipid disorders by promoting mature SREBPs degradation via the ubiquitin-proteasome system. *Theranostics.* 2019;9:5769-83. DOI PubMed PMC
23. Kuan YC, Hashidume T, Shibata T, et al. Heat shock protein 90 modulates lipid homeostasis by regulating the stability and function of sterol regulatory element-binding protein (SREBP) and SREBP cleavage-activating protein. *J Biol Chem.* 2017;292:3016-28. DOI PubMed PMC
24. Mirhadi E, Butler AE, Kesharwani P, Sahebkar A. Utilizing stimuli-responsive nanoparticles to deliver and enhance the anti-tumor effects of bilirubin. *Biotechnol Adv.* 2024;77:108469. DOI PubMed
25. Bortolussi G, Shi X, Ten Bloemendaal L, et al. Long-term effects of biliverdin reductase a deficiency in *ugt1-/-* mice: impact on redox status and metabolism. *Antioxidants.* 2021;10:2029. DOI PubMed PMC
26. Li Y, Huang B, Ye T, Wang Y, Xia D, Qian J. Physiological concentrations of bilirubin control inflammatory response by inhibiting NF-κB and inflammasome activation. *Int Immunopharmacol.* 2020;84:106520. DOI PubMed
27. Bianco A, Dvořák A, Capková N, et al. The extent of intracellular accumulation of bilirubin determines its anti- or pro-oxidant effect. *Int J Mol Sci.* 2020;21:8101. DOI PubMed PMC
28. Vitek L, Hinds TD Jr, Stec DE, Tiribelli C. The physiology of bilirubin: health and disease equilibrium. *Trends Mol Med.* 2023;29:315-28. DOI PubMed PMC
29. Adin CA. Bilirubin as a therapeutic molecule: challenges and opportunities. *Antioxidants.* 2021;10:1536. DOI PubMed PMC
30. Gordon DM, Hong SH, Kipp ZA, Hinds TD Jr. Identification of binding regions of bilirubin in the ligand-binding pocket of the peroxisome proliferator-activated receptor-A (PPARalpha). *Molecules.* 2021;26:2975. DOI PubMed PMC
31. Kim TW, Kim Y, Jung W, et al. Bilirubin nanomedicine ameliorates the progression of experimental autoimmune encephalomyelitis by modulating dendritic cells. *J Control Release.* 2021;331:74-84. DOI PubMed
32. Tomaro ML, Batlle AM. Bilirubin: its role in cytoprotection against oxidative stress. *Int J Biochem Cell Biol.* 2002;34:216-20. DOI PubMed
33. Yang K, Battista C, Woodhead JL, et al. Systems pharmacology modeling of drug-induced hyperbilirubinemia: differentiating hepatotoxicity and inhibition of enzymes/transporters. *Clin Pharmacol Ther.* 2017;101:501-9. DOI PubMed PMC